

The chromospheric emission from acoustically heated stellar atmospheres

P. Ulmschneider

Institut für Theoretische Astrophysik, Universität Heidelberg, Im Neuenheimer Feld 561,
D-6900 Heidelberg, Federal Republic of Germany

Received August 26, 1988; accepted February 21, 1989

Summary. General properties of acoustically heated chromospheres of late-type stars are derived. For a giant ($\log g = 3$) and a dwarf star ($\log g = 5$) of $T_{\text{eff}} = 5012$ K detailed acoustically heated chromosphere models are constructed and the theoretical Mg II and Ca II emission line fluxes are evaluated. The initial acoustic wave flux in the giant is assumed to be eight times larger than that of the dwarf. The computations show that due to photospheric radiation damping and the limiting shock strength behaviour, the acoustic flux decreases much more rapidly in the giant than in the dwarf star such that roughly the same theoretical emission line fluxes are produced in both stars. This agrees with observations and removes a major argument against the acoustic heating theory for chromospheres of slowly rotating stars.

Key words: hydrodynamics – shocks – stellar chromospheres – chromospheric line emission

1. Introduction

It appears now generally accepted that the emission flux in chromospheric lines and transition region lines of Ca II, Mg II, Si II and C II, all exhibit colour-dependent intrinsic minima. For a recent display of such lower limits see Schrijver (1987b). It seems that both dwarf and giant stars have the same minimum emission. For Ca II Rutten (1986, Fig. 1 curve 5) suggested that this lower limit may not be due to the chromospheric emission but rather to the photospheric background. Careful high resolution analysis of the photospheric background in the centers of the Ca II H and K lines of 16 old stars (Marilli et al., 1989) lying near the minimum emission flux limit showed however, that Rutten's estimate of the photospheric background is too high. Marilli et al. moreover demonstrated that a considerable gap exists between the limiting Ca II emission flux and the flux due to the photospheric background in radiative equilibrium. This confirms that the lower limit of the chromospheric emission flux is indeed an intrinsic property of late type stars.

Several authors (e.g. Golub, 1983; Noyes et al., 1984; Hartmann et al., 1984; Simon et al., 1985; Marilli et al., 1986, 1988; Rutten, 1986) have shown that for late-type stars there is a strong correlation between chromospheric or coronal emission and rotation which can be explained by a greater magnetic flux generation in more rapidly rotating stars and by the observed

correlation between magnetic flux and chromospheric emission for the sun (see e.g. Schrijver and Coté, 1987). For a given spectral type the minimum chromospheric emission flux occurs in stars with large rotation periods. Oranje and Zwaan (1985), Oranje (1986) and Schrijver (1987a, b) have argued that the limiting chromospheric emission flux does not result from the magnetic field related activity, but constitutes a basal chromospheric flux produced by an acoustically heated atmosphere. For late-type stars the acoustic energy generation in magnetic field free regions depends only on the properties of the convection zone layers close to the stellar surface and is thus independent of rotation.

To isolate the magnetic field related activity Oranje and Zwaan (1985), Oranje (1986) and Schrijver (1987a, b) subtract the empirically determined supposedly non-magnetic basal flux values from the observed flux. The increased correlation found between the thus constructed chromospheric excess fluxes of lines and the X-ray emission has recently been disputed by Rutten et al. (1989). Rutten et al. claim that the subtraction of a minimum flux except for Ca II does not improve the correlation between lines, and that a minimum X-ray flux should have also been considered. They argue that the minimum emission constitutes a minimum of magnetic activity and is not a non-magnetic basal flux.

In principle a magnetic versus non-magnetic heating argument should not be based on correlations between chromospheric emission or X-ray fluxes because the correlation between e.g. Ca II and Mg II emission fluxes is due to the fact that the chromosphere is a high temperature layer overlying a colder photosphere and that we see roughly the same hot layer in both lines. Clearly it does not matter whether the chromosphere is heated magnetically or non-magnetically to obtain a correlation between the line emissions. In addition there is no a priori reason to suppose that coronae (and thus X-ray emission) can only be produced by magnetic field related heating. As a matter of fact solar acoustic wave calculations all show steep transition-layer-like temperature rises at the top of the models which points to the reality of purely acoustically heated coronae (Schmitz et al., 1985; Ulmschneider et al., 1987).

In practice, however, X-ray emission always seems to indicate magnetic fields. It is well known that solar X-ray emission is strongly correlated with coronal magnetic loops (see e.g. Vaiana and Rosner, 1978; Rosner et al., 1985). Using the X-ray flux value from solar coronal holes Schrijver (1987b, Fig. 6) shows that the apparent minimum X-ray emission boundary in Fig. 1g of

Rutten et al. (1989) is instrumental and does not constitute an intrinsic basal flux limit. In addition, simple theoretical arguments presented below show that a purely acoustically generated solar corona should have only weak X-ray emission. See also Stepien and Ulmschneider (1989). Thus X-ray emission appears indeed to be a good indicator for magnetic activity and the correlation with chromospheric emission should be a valid tool to disentangle magnetic and non-magnetic heating. This points to the reality of an intrinsic basal chromospheric flux which arises independently from magnetic fields and is generated by acoustic heating.

A serious problem with the acoustic heating theory to explain the basal chromospheric emission flux is the large gravity dependence found in all acoustic energy generation calculations made to date (e.g. Renzini et al., 1977; Fontaine et al., 1981; Bohn, 1984). As mentioned above, this gravity dependence is clearly not seen in the observed chromospheric emission fluxes and has been taken as prime evidence against acoustic heating (Basri and Linsky, 1979; Schrijver, 1987b).

In the present work I want to investigate this gravity dependence argument in more detail. In Sect. 2 the reason for the large gravity dependence found in the acoustic energy flux calculation is discussed. It is well known that a comparison between acoustic fluxes from the top of the convection zone with emission fluxes from chromospheric heights is incorrect, because the influence of the intermediate layers must be taken into account. The intermediate photospheric layers indeed strongly influence the acoustic flux through the process of *radiation damping*, as shown by Ulmschneider (1988). He found that giant stars suffer much more from radiation damping than dwarfs. The present work shows that *shock formation* is another important process by which the acoustic flux in giants decays more rapidly than in dwarfs. This suggests that the gravity dependence argument can no longer be used as evidence against the acoustic heating theory.

For our investigation two theoretical stellar models with $\log g = 5$ (for a dwarf star) and $\log g = 3$ (for a giant) with the same effective temperature $T_{\text{eff}} = 5012$ K were chosen. The acoustic wave calculations for the two stars and the simulations of the Mg II and Ca II line profiles are discussed in Sect. 3. Section 4 gives the results and a discussion while Sect. 5 summarizes the conclusions.

2. Acoustic wave generation

In this section I want to discuss why the acoustic wave generation computations all show a relatively large gravity dependence. In late-type stars with efficient convection zones it is expected that acoustic wave energy is amply generated by the turbulent convection. Renzini et al. (1977) and Fontaine et al. (1981) have used the Lighthill (1952, 1954) formula for quadrupole sound generation developed for homogeneous isotropic turbulence in non-gravitational atmospheres to estimate the emergent acoustic flux at the top of the convection zone of stars. These computations show that the acoustic flux F_M is essentially proportional to g^{-1} , where g is the gravitational acceleration at the stellar surface.

In order to take into account the density stratification found in gravitational atmospheres Bohn (1981, 1984) employed Stein's (1967) method and used improved opacities as well as a better treatment of molecules. He found that due to the contributions from dipole and monopole sound generation terms the gravity dependence of the acoustic energy generation is changed and that

F_M is now proportional to $g^{-0.5}$. For stars where the convection zone is not too thin his results can be represented by the convenient analytical approximation

$$F_M = 1.41 \cdot 10^{26} T_{\text{eff}}^{9.75} g^{-0.5} \alpha^{2.8}, \quad (1)$$

where α is the ratio of mixing-length to pressure scale height.

All this above-mentioned work has recently been criticized by P. Goldreich (1987, private communication) who claims that by using Lighthill's approach (which is developed for non-gravitational atmospheres) in stellar atmospheres, the effect of the buoyancy forces on the turbulence was not properly taken into account. This would mean that in the above computations the quadrupole contribution is overestimated and the dipole contribution is underestimated.

Despite this criticism, however, it is clear from very general arguments that the acoustic energy generation must show a considerable gravity dependence. To show this, convenient approximate formulae for the density ρ , gas pressure p and mean convective velocity v at the top of the convection zone are derived. For these estimates a simple opacity formula

$$\kappa = 1.376 \cdot 10^{-23} p^{0.738} T^5 \text{ (cm}^2/\text{g)}, \quad (2)$$

is used, valid if H^- is the dominant opacity, which was obtained by a fit to the Kurucz (1979) opacity tables (cf. Ulmschneider et al., 1978). Following Renzini et al. (1977) the equation of hydrostatic equilibrium can be integrated down to optical depth $\tau = 1$ under the assumption that the temperature is essentially equal to T_{eff} . For the top of the convection zone one approximately obtains

$$p \simeq 1.96 \cdot 10^{13} g^{0.575} T_{\text{eff}}^{-2.88}, \quad (3)$$

and with the equation of state and a mean molecular weight $\mu = 1.3$

$$\rho \simeq 3.06 \cdot 10^5 g^{0.575} T_{\text{eff}}^{-3.88}. \quad (4)$$

For an efficient convection zone the convective flux

$$F_C = \rho c_p \Delta T v = \rho v^3 \frac{2\gamma}{\alpha(\gamma-1)} \simeq \sigma T_{\text{eff}}^4, \quad (5)$$

must be equal to the total flux. Here the second equality comes from the fact that ΔT and v are related in the mixing-length theory (cf. Renzini et al., 1977). Note that for earlier type stars the last equality in Eq. (5) will not be very good as these convection zones are not very efficient (Cox and Giuli, 1968, p. 609). With the upper limit $\gamma = 5/3$ and with Eq. (4) the mean convective velocity v at the top of the convection zone can be written approximately as

$$v \simeq 3.33 \cdot 10^{-4} \alpha^{0.333} g^{-0.192} T_{\text{eff}}^{2.62}. \quad (6)$$

For monopole, dipole and quadrupole source terms (Stein, 1981) one thus finds approximately

$$F_M^{\text{mono}} \sim \sigma T_{\text{eff}}^4 \left(\frac{v}{c}\right)^1 \sim g^{-0.19} T_{\text{eff}}^{6.1}, \quad (7)$$

$$F_M^{\text{dip}} \sim \sigma T_{\text{eff}}^4 \left(\frac{v}{c}\right)^3 \sim g^{-0.58} T_{\text{eff}}^{10.4}, \quad (8)$$

$$F_M^{\text{quad}} \sim \sigma T_{\text{eff}}^4 \left(\frac{v}{c}\right)^5 \sim g^{-0.96} T_{\text{eff}}^{14.6}, \quad (9)$$

where c is the sound speed. It is seen that except for the monopole

case there is a considerable gravity dependence of the acoustic energy generation. If the dipole contribution is enhanced as suggested by the criticism of Goldreich, then the gravity dependence of Eq. (1) found by Bohn (1981, 1984) should give reasonable estimates for our purpose. Stars differing by a factor of 100 in gravity are thus expected to have acoustic fluxes different by about a factor of ten. The gravity dependence of the acoustic energy generation calculations essentially arises from the steep velocity dependence of the source terms and the fact that in order to transport the total stellar flux σT_{eff}^4 in an effective convection zone, much higher velocities are necessary in the low density surface layers of giants as compared to those of dwarfs.

3. Acoustically heated chromospheres for two stars

In this Sect., I describe the computation of acoustically heated chromosphere models and show the method by which the emergent theoretical Mg II and Ca II emission line flux is calculated.

3.1. Theoretical chromosphere models

For the two stars with $T_{\text{eff}} = 5012$ K and $\log g = 3$ (henceforth called giant) and $\log g = 5$ (henceforth called dwarf) initial grey plane-parallel radiative equilibrium models have been computed which cover roughly seven decades in optical depth τ at 5000 Å up to $\tau = 1.0$. Acoustic waves are calculated by solving the time-dependent continuity, Euler and energy equations in a lagrangian frame using the modified characteristics method described by Ulmschneider et al. (1977, 1978). For the energy balance the radiative transfer and statistical rate equations for the non-grey H^- continuum and the Mg II k line (with complete redistribution, CRD) were solved (see Ulmschneider et al., 1987). Acoustic waves are introduced at the lowermost height point into the atmosphere models by a piston moving sinusoidally in time with a wave period P and a velocity amplitude

$$u_0 = \left(\frac{2F_{M_0}}{\rho c} \right)^{1/2}, \quad (10)$$

where F_{M_0} is the initial acoustic flux generated by the convection zone. ρ is the density and c the sound speed at the bottom of the atmosphere. At the top of the atmosphere a transmitting boundary was assumed. For the giant star an acoustic flux of $F_{M_0} = 2.0 \cdot 10^8$ erg/cm²s and for the dwarf star of $F_{M_0} = 2.5 \cdot 10^7$ erg/cm²s were taken following Bohn (1984, Fig. 6). As discussed above, these values may be uncertain in magnitude but display a realistic gravity dependence. For the wave period P , values

$$P = \frac{1}{10} P_A = \frac{1}{10} \frac{4\pi c}{\gamma g}, \quad (11)$$

much smaller than the acoustic cut-off period P_A were taken. These periods are close to the peak of the acoustic power spectrum computed by Bohn (1981, 1984) and ensure that the waves are propagating. For the giant star one finds $P = 560$ s and for the dwarf star, $P = 5.6$ s. To obtain realistic radiative equilibrium models, time-dependent computations without waves were made, holding the piston position constant by taking $u_0 = 0$.

3.2. Mg II k and Ca II K line computations

In the time-dependent wave computations using the core-saturation method (Kalkofen and Ulmschneider 1984) one evaluates a non-LTE line source function S^L for Mg II or Ca II under the complete redistribution (CRD) approximation. The error made in using this approximation has been discussed by Ulmschneider et al. (1987) and is especially large at great depth because there the coherent emission in the line wing is poorly described by CRD. This line source function S^L has been used to compute the emergent line profile. With a table of background opacities κ^B at the frequencies of the Mg II k or Ca II K lines generated from the ATLAS code of Kurucz (1970) the total source function is given by

$$S = (\kappa_v^L S^L + \kappa^B B) / (\kappa_v^L + \kappa^B), \quad (12)$$

where κ_v^L is the monochromatic line opacity and B the source function in LTE of the background. Evaluating the emergent flux by integrating S over the total optical depth using three point interpolation parabolas (Kalkofen and Ulmschneider 1977) or two point interpolation formulas as described by Kalkofen and Ulmschneider (1984) gave almost identical results.

In the framework of the core-saturation method this procedure to compute the emergent Mg II or Ca II line profiles can be improved to include coherence (PRD) by using the method of Stenholm and Wehrse (1984). Here the core-wing diagram (cf. Kalkofen and Ulmschneider, 1984) has been used as well as the redistribution function after Gouttebroze (1986).

4. Results and discussion

4.1. The stellar models

The radiation hydrodynamic wave computations in the dwarf and giant stars are shown in Figs. 1, and 2, respectively, as function of eulerian height. In both cases the computations have been continued for a long time such that the transient behaviour, arising from the fact that initially the wave runs into an undisturbed radiative equilibrium atmosphere, has been much reduced. At the time of Fig. 1, 210 shocks and at Fig. 2, 19 shocks have been transmitted through the top of the atmosphere. In addition in the dwarf none and in the giant 6 shocks have vanished due to overtaking by other shocks.

It is readily seen that the height scales in both figures are very different, that of the giant being 100 times greater. This results from our choice of a similar optical depth range for both stars. Integrating the hydrostatic equation to the optical depth τ and using Eq. (2) it can be shown (cf. Renzini et al., 1977) that $d\tau/\tau = -1.7dx/H$, where x is the geometrical height and H the scale height. As $H = RT/\mu g$ (where R is the gas constant) is 100 times greater, going from the dwarf to the giant, the heights dx must be likewise. Note that the mass column density of the bottommost point in the giant ($m = 26$ g/cm²) is much larger than that of the dwarf ($m = 3.7$ g/cm²). This is due to the pressure dependence of the opacity. In the dwarf the pressure and the opacity rise quickly and optical depth unity is reached after going through much less mass. The pressures $p = mg$ at the bottom of the atmospheres agree roughly with the approximate values from Eq. (3). With a similar integration of the hydrostatic equation as above one finds $d\tau/\tau = 0.575dp/p = 0.575dm/m$, which shows that the mass column density and the pressure change only by about 4 decades for the chosen optical depth range.

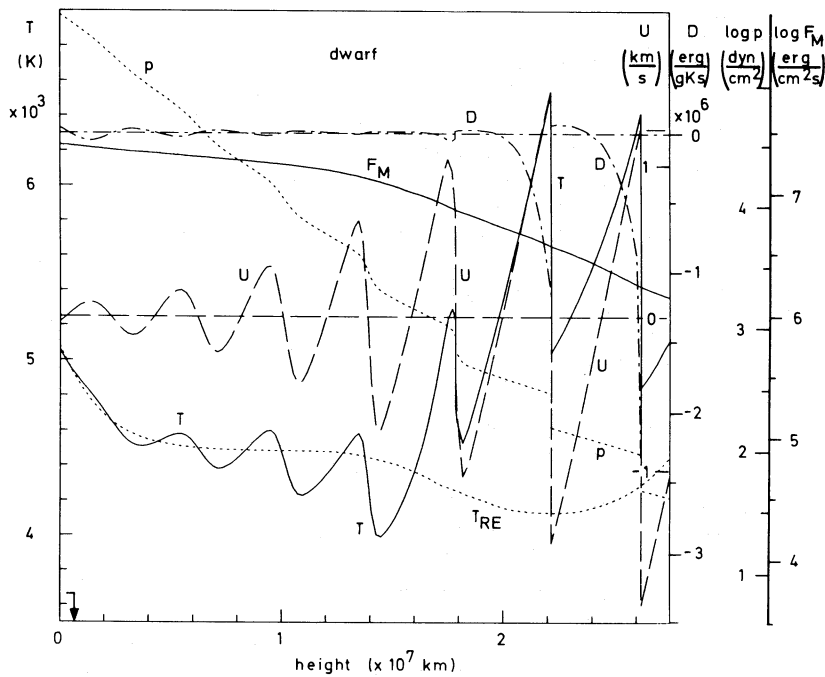


Fig. 1. Acoustically heated theoretical chromosphere model of a dwarf star with $T_{\text{eff}}=5012$ K and $\log g=5$ at time $t=1.22 \cdot 10^3$ s. The temperature T , velocity u , gas pressure p , damping function D and acoustic flux F_M are shown as function of height. T_{RE} is the temperature distribution of a radiative equilibrium model. The acoustic wave has an initial flux of $F_{M_0}=2.5 \cdot 10^7 \text{ erg cm}^{-2} \text{ s}^{-1}$ and a period $P=5.6$ s. The upper end of the radiative damping zone is indicated by an arrow

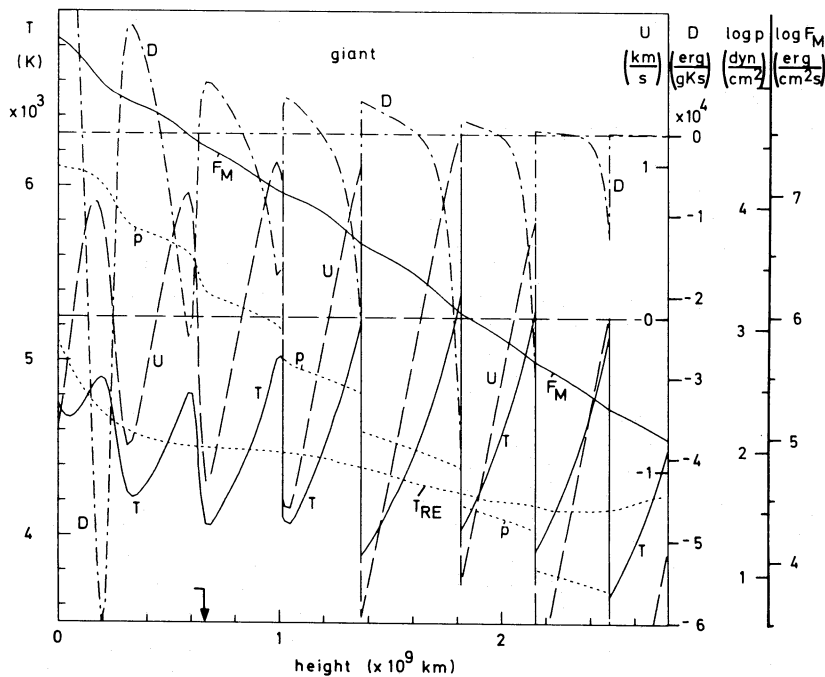


Fig. 2. Acoustically heated theoretical chromosphere model of a giant star with $T_{\text{eff}}=5012$ K and $\log g=3$ at time $t=1.91 \cdot 10^4$ s. The temperature T , velocity u , gas pressure p , damping function D and acoustic flux F_M are shown as function of height. T_{RE} is the temperature distribution of a radiative equilibrium model. The acoustic wave has an initial flux of $F_{M_0}=2.0 \cdot 10^8 \text{ erg cm}^{-2} \text{ s}^{-1}$ and a period $P=560$ s. The upper end of the radiative damping zone is indicated by an arrow

4.2. Limiting shock strength behaviour

Despite the fact that the giant has a 100 times larger height scale as compared to the dwarf it is seen from Figs. 1 and 2 that there are roughly the same number of wavelengths in both atmospheres. This is due to the fact that after Eq. (11) the wave period and thus the wavelength in the giant is increased by the same factor of 100. It is seen that the velocity amplitude at the bottom of the giant atmosphere ($u_0=7 \cdot 10^4$ cm/s) is much larger than the corresponding velocity amplitude in the dwarf ($u_0=9 \cdot 10^3$ cm/s).

This is due to the factor of 8 difference in the acoustic flux. The velocities are in agreement with Eq. (10) if the different densities ($\rho_1=7.8 \cdot 10^{-8}$ and $1.1 \cdot 10^{-6} \text{ g/cm}^3$) are considered.

Figure 1 shows that at greater height soon after the shock becomes fully developed the shock amplitudes tend to reach a constant value. The same is seen even more clearly in Fig. 2. This general behaviour is found in all of our acoustic wave computations (e.g. Ulmschneider et al., 1978, 1979), and is a consequence of the *limiting shock strength behaviour* of acoustic waves. It is well known from early wave calculations (e.g. Osterbrock,

1961; Ulmschneider, 1970; see also Cuntz and Ulmschneider, 1988) that the strength of weak monochromatic acoustic shock waves in gravitational atmospheres attains a limiting value, where the increase of the wave amplitude due to energy conservation in the decreasing density is balanced by the amplitude decay due to shock dissipation.

The surprising result as seen from Figs. 1 and 2 is, however, that the limiting shock amplitudes are the *same* in both dwarf and giant stars. It appears that a fixed limiting shock strength is reached independent of the gravity of the star. This can be explained as follows. The shock Mach number M_s and the shock strength α are defined as

$$M_s \equiv 1 + \alpha \equiv \frac{U_{SH} - u_1}{c_1}, \quad (13)$$

where U_{SH} is the shock speed, u_1 the gas velocity and c_1 the sound speed in front of the shock (Landau Lifshitz, 1959, p. 331). Then with

$$\Phi \equiv \frac{p_2}{p_1} = \frac{2\gamma M_s^2 - \gamma + 1}{\gamma + 1}, \quad (14)$$

$$\Theta \equiv \frac{\rho_2}{\rho_1} = \frac{(\gamma + 1)M_s^2}{(\gamma - 1)M_s^2 + 2}, \quad (15)$$

the temperature, pressure and velocity jumps across the shocks for weak shocks ($\alpha < 1$) are given by

$$\frac{T_2 - T_1}{T_1} = \frac{\Phi}{\Theta} - 1 \simeq \alpha, \quad (16)$$

$$\frac{p_2 - p_1}{p_1} = \Phi - 1 \simeq \frac{4\gamma\alpha}{\gamma + 1}, \quad (17)$$

$$\frac{u_2 - u_1}{c_1} = \frac{\Theta - 1}{\Theta} M_s \simeq \frac{4\alpha}{\gamma + 1}. \quad (18)$$

For the case of plane-parallel isothermal atmospheres with constant gravity the limiting shock strength M_s^{LIM} can be written (Ulmschneider, 1970) as

$$M_s^{LIM} = 1 + \frac{\gamma g}{4c}. \quad (19)$$

A recent discussion of this formula for applications to late-type stellar atmospheres has been given by Cuntz and Ulmschneider (1988).

From a comparison of Eqs. (11) and (19) (here small differences in the sound speeds are neglected) we find for propagating shock waves in late-type stars

$$M_s^{LIM} = 1 + \frac{\pi}{10} \simeq 1.3, \quad (20)$$

independent of T_{eff} and gravity. From Eqs. (16) to (18) the total temperature, pressure and velocity jumps in those weak shock waves are given by

$$\frac{\Delta T}{T} \simeq 0.3, \quad \frac{\Delta p}{p} \simeq 0.75, \quad \frac{\Delta u}{c} \simeq 0.45, \quad (21)$$

likewise independent of T_{eff} and g . With $T_1 = 4500$ K and a sound speed of 7 km/s one finds $\Delta T = 1350$ K and $\Delta u = 3.1$ km/s in good agreement with the values in Figs. 1 and 2.

It should be noted that the general results of Eqs. (20) and (21) rest on the assumptions about the acoustic frequency spectrum made in Eq. (11) and on the validity of Eq. (19) for the limiting shock strength. The computations of Bohn (1981, 1984) have shown that the peak of the acoustic spectrum near $P_A/10$ does not change very much when going through the HR-diagram except for very late type dwarf stars, where Bohn finds a strong monopole contribution which leads to spectra which peak at longer wave period. However, the recent criticism of Goldreich mentioned above might lead to a greater dipole contribution which would shift the peak of the spectrum back to shorter wave periods. If that peak does not occur at $P = P_A/10$ but rather at $P = P_A/5$, then a shock strength of $M_s^{LIM} \simeq 1.6$ is found and the values in Eq. (21) are increased by a factor of 2. This shows the well known fact that larger wave periods lead to stronger shocks. The validity of Eq. (19) has been discussed by Cuntz and Ulmschneider (1988) where it was found (cf. their Fig. 4) that for short period waves (i.e. $P = P_A/10$) this expression is quite good. Thus it is to be expected that a more detailed time-dependent computation of the shock development of an acoustic spectrum will not greatly modify the results of Eq. (21) for the lower and middle chromosphere of stars (where Mg II is emitted). However, if more extended outer atmospheres are considered, then the overtaking of shocks and the formation of very strong, long period shock waves have to be taken into account as demonstrated by Cuntz (1987).

4.3. Acoustic fluxes of limiting strength shock waves

Using the somewhat differently defined shock strength $\eta \equiv (\rho_2 - \rho_1)/\rho_1 \simeq 4\alpha/(\gamma + 1)$ the mechanical flux in weak acoustic saw-tooth shock waves can be written (Ulmschneider, 1970) as

$$F_M = \frac{4\gamma}{3(\gamma + 1)^2} p c \alpha^2. \quad (22)$$

With c and α roughly constant this shows that at greater heights the acoustic fluxes as seen in Figs. 1 and 2 simply scale like the mean gas pressures. In particular, for typical chromospheric conditions we find roughly $F_M \simeq 2.3 \cdot 10^4 p$. From the scaling of the pressure relative to τ as discussed above, or from Figs. 1 and 2, it is seen that the giant has about a factor of ten smaller gas pressure at similar optical depths. Thus at the top of the atmosphere the limiting acoustic flux in the giant is about a factor of ten less than that in the dwarf. Note, that the giant initially had eight times more acoustic flux.

The limiting acoustic fluxes decrease rapidly and at the foot of the transition layer reach rather small values. This can be seen in the solar case. With a transition layer pressure of $p = 0.15$ dyn/cm², a sound speed $c = 9$ km/s and $\alpha = 0.3$ one finds from Eq. (22) $F_M = 3.8 \cdot 10^3$ erg/cm² s. This is about two orders of magnitude smaller than the observed solar coronal energy losses (cf. Athay, 1976, p. 423). The X-ray flux which would be generated by this limiting acoustic flux is even smaller. Using values from Withbroe and Noyes (1977) for coronal holes one finds that the fraction of the acoustic flux available for X-rays is only 1/80 of the total coronal energy loss which consists of X-ray-, wind- and conductive losses. Thus the X-ray flux from a purely acoustically heated sun could be as low as 50 erg/cm² s.

A note of caution has to be introduced here. The above arguments are valid for monochromatic wave propagation. To replace the acoustic spectrum by a delta function at the peak of

the acoustic power is very likely permissible when considering chromospheric wave propagation. However, when discussing higher layers the overtaking of shocks as found by Cuntz (1987) will lead to a shift of the acoustic power to much longer period. As longer wave periods after Eqs. (19) and (22) lead to higher limiting fluxes, the expected acoustic fluxes available for X-ray losses very likely are considerably larger than those estimated above. Nevertheless, these arguments show that purely acoustically heated coronae probably have little X-ray emission.

4.4. Radiation damping

There are two processes which are responsible for the differential loss of about a factor of 100 in mechanical flux from the giant. The first process as discussed in the last section is the *limiting shock strength behaviour*. This process generates acoustic waves of limiting strength independent of the initial wave amplitude. If the wave initially has too much energy then shock dissipation reduces the wave amplitude until the limiting value is reached. Likewise if the wave initially has little energy then the steepening by the density gradient will raise the amplitude until the limiting shock strength is reached. As discussed above the acoustic fluxes of limiting strength waves scale essentially like the gas pressure p .

The second process for the large loss of mechanical energy in the giant is *radiation damping*. This effect has been discussed by Ulmschneider (1988). The action of radiation damping is readily seen in Figs. 1 and 2. In the dwarf (Fig. 1) the acoustic wave does not suffer much from radiation damping and the wave amplitude grows quickly due to energy conservation. That the acoustic energy at low heights is roughly conserved is seen from the behaviour of the acoustic flux F_M . In the giant (Fig. 2), however, the large amplitude of the wave entering at the bottom due to strong radiation damping does not grow despite the rapid drop

in density. Here the acoustic flux decays rapidly with height. The zone of the star where radiation damping is important is the region where the wave period P is larger than the radiative relaxation time t_{rad} which is defined (Schmitz, 1989) by

$$t_{\text{rad}} = \frac{2.5c_v}{16\sigma\kappa T^3}, \quad (23)$$

where c_v (erg/g K) is the specific heat at constant volume. A wave with $t_{\text{rad}} \ll P$ will suffer strongly from radiation damping (cf. Ulmschneider, 1988) while a wave with $t_{\text{rad}} \gg P$ will conserve energy. The fact that stars have extensive radiation damping zones has been discussed elsewhere (Ulmschneider et al., 1979; Schmitz and Ulmschneider, 1981). The radiative damping zones extend from the stellar surface where $t_{\text{rad}} \ll P$ up to those heights where $t_{\text{rad}} = P$ and are marked by arrows in Figs. 1 and 2. At the bottom of the atmospheres we find $t_{\text{rad}} = 3.5$ s for the dwarf ($P = 5.6$ s) and $t_{\text{rad}} = 29$ s for the giant ($P = 500$ s). The different ratio t_{rad}/P and the different extent of the damping zones show that the acoustic waves in the giant suffer much more from radiation damping than in the dwarf. This behaviour can be understood from the gravity dependence of the ratio P/t_{rad} as discussed by Ulmschneider (1988). Radiation damping strongly influences the acoustic flux in the radiation damping zones but does not modify the magnitude of the flux of limiting shock waves found at great heights.

4.5. The emerging Mg II k and Ca II K line profiles

For the atmospheric slabs given by Figures. 1 and 2 the resulting Mg II k and Ca II K line profiles of the dwarf and the giant stars are shown in Figs. 3 to 6. In addition these Figs. show Mg II and Ca II line profiles for the radiative equilibrium models (i.e. the

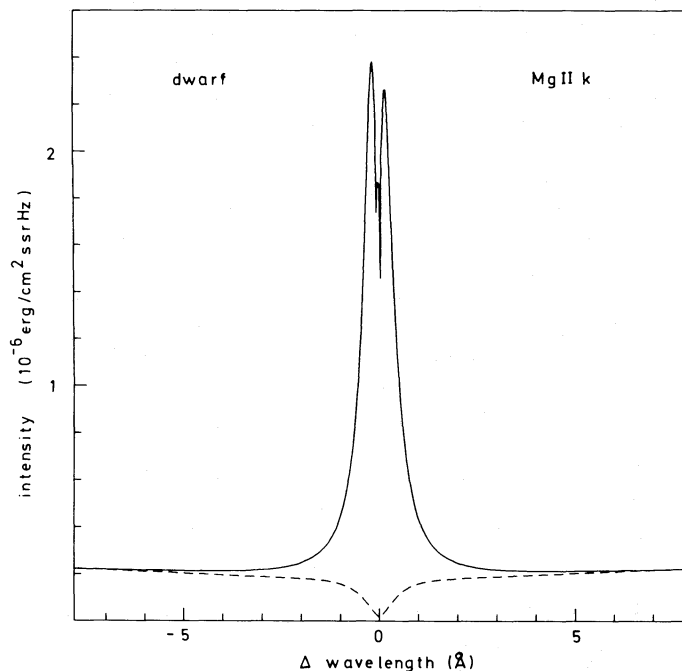


Fig. 3. Mg II k line profiles for the dwarf star in the phase given by Fig. 1. The profile of the radiative equilibrium model is shown dashed

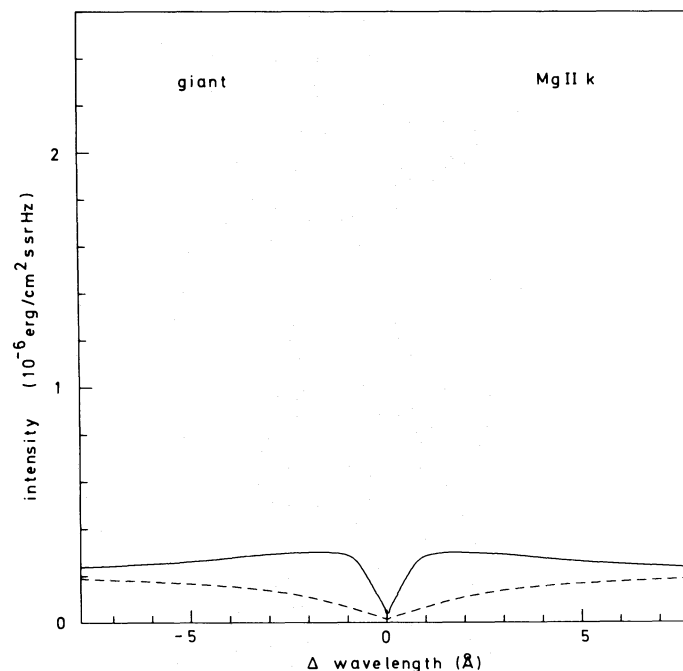


Fig. 4. Mg II k line profiles for the giant star in the phase given by Fig. 2. The profile of the radiative equilibrium model is shown dashed

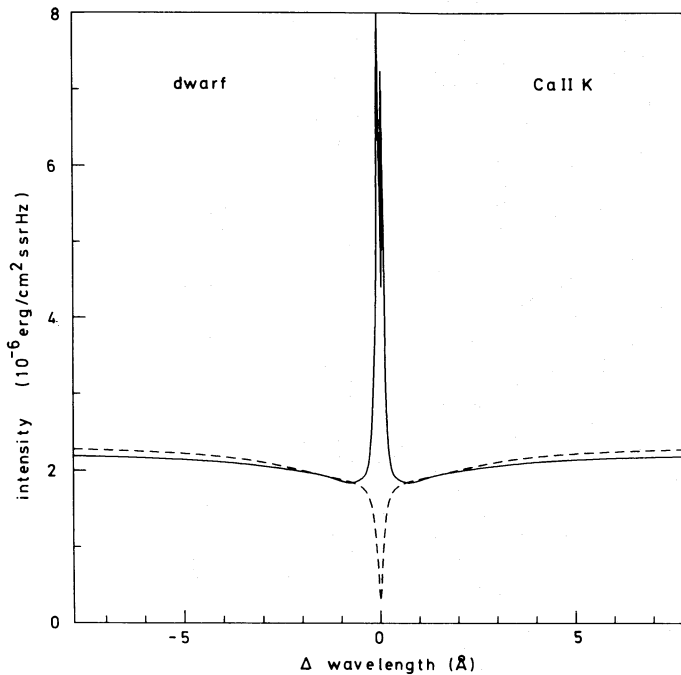


Fig. 5. Ca II K line profiles for the dwarf star in the phase given by Fig. 1. The profile of the radiative equilibrium model is shown dashed

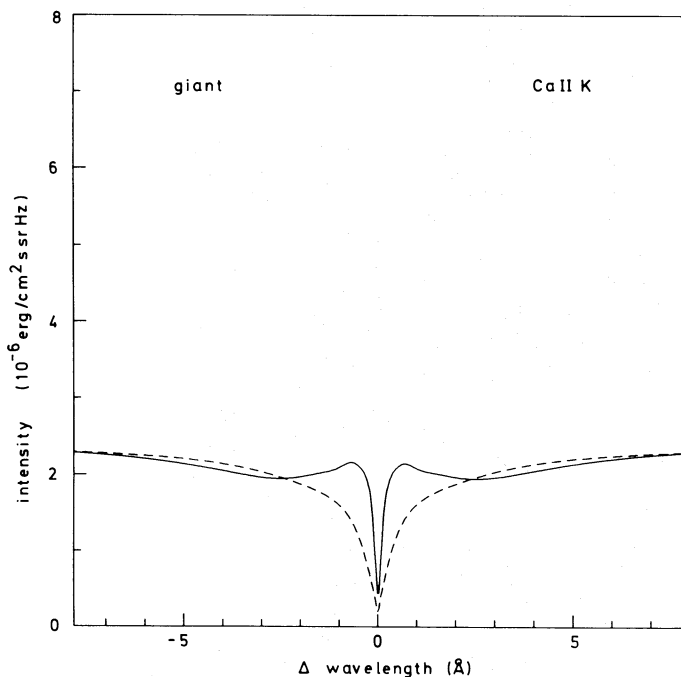


Fig. 6. Ca II K line profiles for the giant star in the phase given by Fig. 2. The profile of the radiative equilibrium model is shown dashed

atmosphere without waves). Note that due to our two level atom description the lines are quite crude and we do not have line doublets but only single lines. The flat appearance and the dependence of the profiles on the wave phase at large $\Delta\lambda$ comes from our slab boundary condition (Ulmschneider et al., 1978, Eqs. 6 and 7, where $\sigma T_{\text{eff}}^4/\pi$ and B_1 were replaced by monochromatic Planck functions). This slab boundary condition does

not take into account deeper photospheric layers. Figures 3 to 6 show that the radiative equilibrium atmospheres produce absorption lines. The emission cores in the lines are therefore generated entirely by the presence of the acoustic waves. This confirms the theoretical picture that the chromospheric line emission from stars is caused by mechanical heating.

The radiative equilibrium models shown in Figs. 1 and 2 were produced by time-dependent means and at great heights very likely have not yet fully settled to a final form, although both models were run for a long time ($4.31 \cdot 10^3$ s for the dwarf and $2.93 \cdot 10^5$ s for the giant). A comparison of the temperature profiles of the atmospheres with and without waves in Figs. 1 and 2 show the well known temperature depression of the wave atmosphere caused by the nonlinearity of the Planck function (cf. Ulmschneider et al., 1978). This temperature depression is also seen in the Ca II profiles of Figs. 5 and 6.

It is interesting to see that for the Mg II lines the chromospheric emission fluxes in the line profiles are roughly similar in both stars, being somewhat smaller in the giant. The Ca II line emission fluxes are likewise roughly similar, although the giant star emission appears noticeably larger. This trend is understood from the fact that the Ca II emission originates deeper in the atmosphere than the Mg II emission. As discussed above we expect that in deeper atmospheric layers the giant star has larger acoustic flux and in higher layers smaller acoustic flux as compared to the dwarf. This near equality of the middle chromospheric emission fluxes has already been expected from the above discussion of the limiting shock strength and radiation damping behaviour. Figures 3 to 6 show that at middle chromospheric heights where the main contribution to the Mg II and Ca II line emission arises, the factor of 8 difference in the initial wave energy is largely dissipated and/or radiated away at other wavelengths (in our case by the H^- continuum). Whether the effect is real, that the giants seem to have a somewhat larger Ca II K but smaller Mg II k emission compared to the dwarfs, must await a more detailed calculation using an acoustic frequency spectrum and a better radiation treatment of the energy equation.

Calculations which simulated line profiles using the partial redistribution (PRD) procedure described above, did not change the line profiles much compared to the CRD profiles. This was attributed to the fact that most of the emission comes from the damping wings of the line at $\Delta\lambda > 0.5 \text{ \AA}$ where the difference between CRD and PRD in the line shape is small (cf. Mihalas, 1978, Fig. 13-8). More detailed line simulations, in view of our approximations as to the Mg II atomic model, the computation of hydrogen ionization for the electron density and the radiation treatment in the hydrodynamics of the wave calculation appeared not warranted at the present time. Such detailed simulations, which can be compared with observed profiles, must await more realistic wave calculations.

5. Conclusions

From the strong velocity dependence of the acoustic dipole and quadrupole source terms we conclude that the acoustic energy generation by turbulent convection in late type stars will show a gravity dependence roughly like $g^{-0.5}$ which leads to much higher acoustic energy fluxes in giants as compared to dwarfs. This is essentially due to the higher convective velocities needed in the low density envelopes of giants in order to transport the same total flux.

It has been shown that there are two processes, *radiation damping* and *the limiting shock strength behaviour* which rapidly decrease the acoustic flux on its transit from the convection zone to the middle and high chromosphere. Radiation damping due to the different gravity dependence of the radiative relaxation time t_{rad} (which essentially does not depend on gravity) and the wave period P (which depends on gravity) affects giants more than dwarfs (see Ulmschneider, 1988). The limiting shock strength reached by acoustic waves in the chromosphere is independent of the initial acoustic energy flux generated in the convection zone and depends essentially on the product gP .

Computations of the generated acoustic frequency spectra show that the peak of the acoustic power is near $P_A/10$, where P_A is the acoustic cut-off period of the atmosphere. As P_A scales like g^{-1} it is shown generally that *the limiting shock strength in all late-type stars is roughly similar*, independent of T_{eff} and gravity. This allows to predict roughly the same temperature, pressure and velocity jumps in limiting acoustic shock waves in late-type stars. As the limiting acoustic flux essentially scales like the gas pressure p , it was concluded that the acoustic flux in the high chromospheres of late-type stars is very weak and probably unable to balance the observed coronal X-ray emission in these stars. This agrees well with the small acoustic fluxes observed for the Sun with the OSO 8 satellite and makes coronal X-ray emission a prime indicator of magnetic heating.

For a giant ($\log g=3$) and a dwarf star ($\log g=5$) of $T_{\text{eff}}=5012$ K detailed acoustically heated chromosphere models were constructed and theoretical emission line profiles evaluated. The initial acoustic wave flux in the giant is assumed to be 8 times larger than that of the dwarf. Despite this initial disparity in the acoustic flux it is found that the Mg II and Ca II line emission fluxes for the two stars are roughly the same. This is attributed to the above mentioned degradation of the acoustic flux by radiation damping and shock dissipation during transit from the convection zone to the middle chromosphere. That the theoretical chromospheric Mg II and Ca II line emission shows little gravity dependence, despite the considerable gravity dependence of the generated initial acoustic flux, removes a main argument against acoustic waves as proposed heating mechanism for the outer atmosphere of the slowly rotating minimum chromospheric emission stars.

Acknowledgement. I want to thank the Deutsche Forschungsgemeinschaft for generous support of project U1 57/11-1.

References

- Athay, R.G.: 1976, *The Solar Chromosphere and Corona: Quiet Sun*, Reidel, Dordrecht
- Basri, G.S., Linsky, J.L.: 1979, *Astrophys. J.* **234**, 1023
- Bohn, H.U.: 1981, Ph.D. thesis, University of Würzburg
- Bohn, H.U.: 1984, *Astron. Astrophys.* **136**, 338
- Cox, J.P., Giuli, R.T.: 1968, *Principles of Stellar Structure*, Vol. 2, Gordon and Breach, New York
- Cuntz, M.: 1987, *Astron. Astrophys.* **188**, L5
- Cuntz, M., Ulmschneider, P.: 1988, *Astron. Astrophys.* **193**, 119
- Fontaine, G., Villeneuve, B., Wilson, J.: 1981, *Astron. Astrophys.* **243**, 550
- Golub, L.: 1983, *Activity in Red-Dwarf Stars*, eds. P.B. Byrne, M. Rodono, Reidel, Dordrecht, p. 83
- Gouttebroze, P.: 1986, *Astron. Astrophys.* **160**, 195
- Hartmann, L.W., Baliunas, S.L., Duncan, D.K., Noyes, R.W.: 1984, *Astrophys. J.* **279**, 778
- Kalkofen, W., Ulmschneider, P.: 1977, *Astron. Astrophys.* **57**, 193
- Kalkofen, W., Ulmschneider, P.: 1984, *Methods in Radiative Transfer*, ed. W. Kalkofen, Univ. Press, Cambridge, p. 131
- Kurucz, R.: 1970, *Smithsonian Astrophys. Obs. Spec. Rep.* **309**
- Kurucz, R.: 1979, *Astrophys. J. Suppl.* **40**, 1
- Landau, L.D., Lifshitz, E.M.: 1959, *Fluid Mechanics*, Pergamon Press, London, p. 331
- Lighthill, M.J.: 1952, *Proc. Roy. Soc.* **A211**, 564
- Lighthill, M.J.: 1954, *Proc. Roy. Soc.* **A222**, 1
- Marilli, E., Catalano, S., Trigilio, C.: 1986, *Astron. Astrophys.* **167**, 297
- Marilli, E., Catalano, S., Trigilio, C.: 1989, *Astron. Astrophys.* (to be published)
- Mihalas, D.: 1978, *Stellar Atmospheres*, Freeman, San Francisco
- Noyes, R.W., Hartmann, L., Baliunas, S.L., Duncan, D.K., Vaughan, A.H.: 1984, *Astrophys. J.* **279**, 763
- Oranje, B.J.: 1986, *Astron. Astrophys.* **154**, 185
- Oranje, B.J., Zwaan, C.: 1985, *Astron. Astrophys.* **147**, 265
- Osterbrock, D.E.: 1961, *Astrophys. J.* **134**, 347
- Renzini, A., Cacciari, C., Ulmschneider, P., Schmitz, F.: 1977, *Astron. Astrophys.* **61**, 39
- Rosner, R., Golub, L., Vaiana, G.S.: 1985, *Ann. Rev. Astron. Astrophys.* **23**, 413
- Rutten, R.G.M.: 1986, *Astron. Astrophys.* **159**, 291
- Rutten, R.G.M., Lemmens, A.F.P., Zwaan, C.: 1989, *Astron. Astrophys.* (to be published)
- Schmitz, F.: 1989, *Astron. Astrophys.* (to be published)
- Schmitz, F., Ulmschneider, P.: 1981, *Astron. Astrophys.* **93**, 178
- Schmitz, F., Ulmschneider, P., Kalkofen, W.: 1985, *Astron. Astrophys.* **148**, 217
- Schrijver, C.J.: 1987a, *Astron. Astrophys.* **172**, 111
- Schrijver, C.J.: 1987b, in *Cool Stars, Stellar Systems and the Sun*, eds. J.L. Linsky, R.E. Stencel, *Lecture Notes in Physics* **291**, Springer, Berlin, Heidelberg, New York, p. 135
- Schrijver, C.J., Coté, J.: 1987, in *Cool Stars, Stellar Systems and the Sun*, eds. J.L. Linsky, R.E. Stencel, *Lecture Notes in Physics* **291**, Springer, Berlin, Heidelberg, New York, p. 51
- Simon, T., Herbig, G.H., Boesgaard, A.M.: 1985, *Astrophys. J.* **293**, 551
- Stein, R.F.: 1967, *Solar Physics* **2**, 385
- Stein, R.F.: 1981, *Astrophys. J.* **246**, 966
- Stenholm, L.G., Wehrse, R.: 1984, *Astron. Astrophys.* **131**, 399
- Stepien, K., Ulmschneider, P.: 1989, *Astron. Astrophys.* **216**, 139
- Ulmschneider, P.: 1970, *Solar Physics* **12**, 403
- Ulmschneider, P.: 1988, *Astron. Astrophys.* **197**, 223
- Ulmschneider, P., Kalkofen, W., Nowak, T., Bohn, H.U.: 1977, *Astron. Astrophys.* **54**, 61
- Ulmschneider, P., Schmitz, F., Hammer, R.: 1979, *Astron. Astrophys.* **74**, 229
- Ulmschneider, P., Schmitz, F., Kalkofen, W., Bohn, H.U.: 1978, *Astron. Astrophys.* **70**, 229
- Ulmschneider, P., Muchmore, D., Kalkofen, W.: 1987, *Astron. Astrophys.* **177**, 292
- Vaiana, G.S., Rosner, R.: 1978, *Ann. Rev. Astron. Astrophys.* **16**, 393
- Withbroe, G.L., Noyes, R.W.: 1977, *Ann. Rev. Astron. Astrophys.* **15**, 363